Uranium(V) incorporation mechanisms and stability in Fe(II)/Fe(III) iron (oxyhydr)oxides

Roberts, H. E.; Morris, K.; Law, G. T. W.; Mosselmans, J. F. W.; Bots, P.; Kvashnina, K.; Shaw, S.;

Originally published:

September 2017

Environmental Science & Technology Letters 4(2017)10, 421-426

DOI: https://doi.org/10.1021/acs.estlett.7b00348

Uranium(V) incorporation mechanisms and stability in Fe(II)/Fe(III) (oxyhydr)oxides

Journal:	*Environmental Science & Technology Letters*
Manuscript ID	ez-2017-00120g
Manuscript Type:	Letter
Date Submitted by the Author:	05-Apr-2017

Complete List of Authors:	Roberts, Hannah; University of Manchester Faculty of Engineering and Physical Sciences, School of Earth and Environmental Sciences Morris, Katherine; The University of Manchester, SEAES Law, Gareth; University of Manchester, Research Centre for Radwatse Disposal mosselmans, julian; Diamond Light Source Ltd., Principal Beamline Scientist Kvashnina, Kristina; ESRF Bots, Pieter; University of Manchester, Civil and Environmental Engineering Shaw, Samuel; University of Manchester, School of Earth, Atmospheric and Environmental Sciences

Uranium(V) incorporation mechanisms and stability in Fe(II)/Fe(III) iron (oxyhydr)oxides

Hannah E. Roberts[a], Katherine Morris[a], Gareth T. W. Law[b], J. Frederick W. Mosselmans[c], Pieter Bots[a1], Kristina Kvashnina[d,e], and Samuel Shaw[a,*]

[a]Research Centre for Radwaste Disposal and Williamson Research Centre for Molecular Environmental Science, School of Earth, Atmospheric and Environmental Sciences, The University of Manchester, Manchester, M13 9PL, United Kingdom; [b]Centre for Radiochemistry Research and Research Centre for Radwaste and Decommissioning, School of Chemistry, The University of Manchester, Manchester, M13 9PL, United Kingdom; [c]Diamond Light Source Ltd, Diamond House, Harwell Science and Innovation Campus, Didcot, Oxfordshire, OX11 0DE, United Kingdom; [d]The Rossendorf Beamline at ESRF – The European Synchrotron, CS40220, 38043, Grenoble Cedex 9, France; [e]Helmholtz Zentrum Dresden-Rossendorf (HZDR), Institute of Resource Ecology, PO Box 510119, 01314 Dresden, Germany. [1]Present address: Department of Civil and Environmental Engineering, University of Strathclyde, Glasgow, G1 1XJ, United Kingdom.

[8]To whom correspondence should be addressed. Email: sam.shaw@manchester.ac.uk

Abstract

Understanding the interactions between radionuclides and mineral phases underpins site environmental clean-up and waste management in the nuclear industry. The transport and fate of radionuclides in many subsurface environmental systems are controlled by adsorption, redox and mineral incorporation processes. Interactions of iron (oxyhydr)oxides with uranium have been extensively studied due to both the abundance of uranium as an environmental contaminant and the ubiquity of iron (oxyhydr)oxides in engineered and natural environments. Despite this, detailed mechanistic information regarding the incorporation of uranium into Fe(II) bearing magnetite and green rust is sparse. Here, we present a co-precipitation study where U(VI) was reacted with environmentally relevant iron(II/III) (oxyhydr)oxide mineral phases. Based on diffraction, microscopic and spectroscopic evidence, we propose the reduction of U(VI) via a one electron transfer to U(V) and stabilisation of the U(V) by incorporation during co-precipitation with iron (oxyhydr)oxides. U(V) was stable in both magnetite and green rust structures and incorporated via substitution for octahedrally coordinated Fe in a uranate-like coordination environment. As the Fe(II)/Fe(III) ratio increased, a proportion of U(IV) was also precipitated as surface associated UO_2. These novel observations have significant implications for the behaviour of uranium within engineered and natural environments.

Uranium | Magnetite | Green Rust | Incorporation | Environmental fate

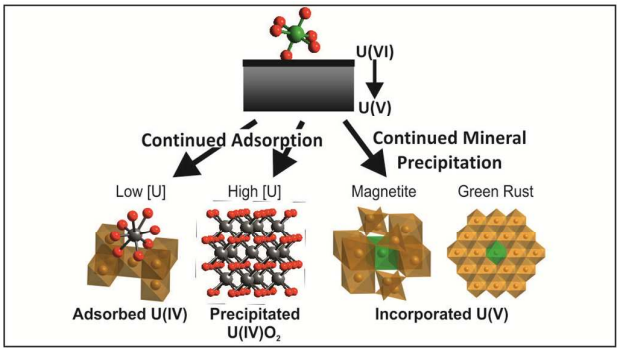

Introduction

Uranium is the dominant radionuclide by mass in many radioactively contaminated land and radioactive waste disposal scenarios. The oxidation state of uranium is a significant control on its subsurface environmental mobility. Under oxic conditions, soluble and

environmentally mobile U(VI) dominates; under anaerobic conditions, uranium is typically reduced to poorly soluble U(IV). In biological and abiotic reduction, U(V) reportedly forms as a transient species during U(VI) reduction and recent work suggests that U(V) may be stabilized at mineral surfaces.[1–7] The potential for U(V) incorporation into environmentally relevant iron (oxyhydr)oxide phases such as magnetite ($Fe^{II}Fe^{III}_2O_4$) has also been shown.[8–12] Indeed, establishing the extent of U(V) stability on interaction with Fe (oxyhydr)oxides is essential in underpinning predictive models for U behavior in environmental systems which currently do not recognise the presence of U(V). To achieve this, the U speciation needs to be determined at a molecular scale which will be essential in defining the significance of U(V) in environmental systems and in developing realistic models to predict the environmental fate of uranium.

Fe(II)/Fe(III) bearing (oxyhydr)oxide minerals such as magnetite and green rust[13] (e.g. $[Fe^{II}_3Fe^{III}(OH)_8]^+$,$[Cl,nH_2O]^-$) are ubiquitous in anoxic subsurface environments (e.g. soils, and sediments), forming via a variety of biogeochemical processes[14,15] and are also formed during the anaerobic corrosion of steel, a significant component in contaminated, engineered environments and geological disposal facilities.[16–18] The pathway of U(VI) reduction at the Fe(II)/Fe(III) (oxyhydr)oxide surface occurs via a two-step process. Firstly, a one electron transfer process leads to the formation of U(V). Secondly, the highly transient U(V) species rapidly disproportionates to form either nanoparticulate uraninite or absorbed, non-crystalline U(IV). Previous studies have suggested that U(V) can be stabilized via its incorporation into bulk magnetite within the octahedral sites, although the exact structural site is yet to be determined, and no information on U(V) stabilisation in other Fe(II)/Fe(III) (oxyhydr)oxide is currently available.[1,9,12] Atomistic simulations of U incorporation into iron (oxyhydr)oxide minerals have suggested that both U(VI) and U(V) have the potential to substitute for octahedrally coordinated Fe within the magnetite structure.[8,19] This is supported by recent spectroscopic studies which suggest that U can be incorporated into the iron oxide mineral structures in a distorted uranate-like coordination which can be adopted by both U(VI) and U(V).[8,9] Recently, advances in spectroscopic techniques have demonstrated that U(IV), U(V) and U(VI) can be distinguished using high resolution XANES techniques. Ultimately, if U(V) is incorporated into the structure of Fe(II)/Fe(III) (oxyhydr)oxides after U(VI) reduction, this could prevent disproportionation and lead to long term immobilisation of U(V). However, the pathway and mechanism of U(V) incorporation into magnetite and green rust are either poorly defined or yet to be determined.

Here, we synthesised both magnetite and green rust with U(VI) via a co-precipitation process. We then gained unprecedented molecular scale insights into the speciation and atomic-scale mechanisms of incorporation of U within the mineral structures by using state-of-the-art high energy resolution fluorescence detected X-ray absorption near edge structure (HERFD-XANES) spectroscopy in combination with extended X-ray absorption fine structure (EXAFS) spectroscopy. Synchrotron analysis unequivocally confirmed the reduction of U(VI) to stabilized, octahedrally coordinated U(V) which is incorporated within both magnetite and green rust. This facile stabilization of U(V) within these bulk mineral phases has important implications for the fate of U in engineered and natural environments where U(V) has typically been considered transient.

Methods

Mineral synthesis and characterisation Uranium bearing magnetite and green rust were synthesized using a direct co-precipitation method with experiments performed at room temperature in an anaerobic chamber.[20] In brief, solutions of 0.1 M $FeCl_2$, 0.2 M $FeCl_3$, 0.3 M HCl and 0.29 mM U(VI) were mixed for 24 hours before mineral precipitation was induced by introduction of the Fe(II)/Fe(III) solution into a N_2 sparged 28-30% w/v NH_4OH solution (pH 11) under continuous stirring over 15 minutes to a final pH of 9. This led to the instantaneous co-precipitation of the uranium doped minerals. Four different starting Fe(II)/Fe(III) ratios were used to form magnetite and green rust:

$$x = \frac{Fe\ (II)_{[OCT]}}{Fe\ (III)_{[OCT]} + Fe(III)_{[TET]}} = 0.5, 0.6, 0.8\ \&\ 2.0$$

After reaction, the solid samples were analyzed by powder X-ray diffraction (XRD) and transmission electron microscopy (TEM) to characterize the structure, particle size and morphology.

X-ray Absorption Spectroscopy (XAS) Uranium L_{III} edge XAS spectra were collected on wet mineral pastes at Diamond Light Source, beamline B18[21] in a liquid N_2 cryostat in fluorescent mode using a Ge detector.[22] Analysis of the EXAFS spectra was performed in Artemis and Athena.[23] U M_4 edge HERFD XANES spectra were collected at European Synchrotron Radiation Facility, beamline ID26[24] through the use of a X-ray emission spectrometer[25,26] and analysed using iterative transformation factor analysis[12,27] to determine the proportion of (UIV), U(V) and U(VI) in the samples.

Results and Discussion

Co-precipitation experiments were performed to determine the speciation of uranium following co-precipitation with either magnetite or green rust. The Fe(II)/Fe(III) (oxyhydr)oxides were co-precipitated with U(VI) at starting Fe(II)/Fe(III) ratios of 0.5/0.6 to synthesise magnetite and 0.8/2.0 to synthesise green rust (Figure S1). Additionally, transmission electron microscopy showed the magnetite was nanoparticulate, with particle sizes ranging from 1 to 20 nm (Figure S2). Green rust was present as pseudo-hexagonal plates of approximately 50 - 600 nm, and energy dispersive X-ray analysis showed chloride was present, indicating green rust chloride formed (Figure S3).

Reduction of U(VI) to stable U(V). Uranium M_4 edge HERFD XANES spectra were used to determine the oxidation state of U associated with the Fe(II)/Fe(III) (oxyhydr)oxide phases (Figure 1).[12,28,29] The energy of the XANES peak position showed a systematic decrease with increasing Fe(II)/Fe(III) ratio (Figure S4) from 3726.5 eV (at 0.5 Fe(II)/Fe(III)) to 3726.3 eV (at 2.0 Fe(II)/Fe(III)). Comparison with the peak position of the U oxidation state standards (U(VI) = 3726.95 eV, U(V) = 3726.4 eV and U(IV) = 3725.2 eV) suggests that U(V) dominated in all of the samples. Furthermore, there were no indications of the higher energy peaks (3728.7 eV and 3732.0 eV) which are typical of the U(VI) uranyl standard. However, in the Fe(II)/Fe(III) = 2.0 spectra, the small shoulder on the low energy side of the XANES spectrum confirms the presence of U(IV) (Fig. 1). Iterative transformation factor analysis (ITFA) of the HERFD-XANES data identified the three main component present in the samples (Figure S5) and indicated that at Fe(II)/Fe(III) = 0.5 – 0.8, 87-96 % of U was present as U(V), with the remainder contributing from U(VI) for Fe(II)/Fe(III) = 0.5 and U(IV) for Fe(II)/Fe(III) = 0.6 and

0.8 (Table S1)). At Fe(II)/Fe(III) = 2.0, U(V) still dominated but the amount of U(IV) had increased to approximately 28 % in this sample. The L_{III}- edge XANES also supports stabilisation of U(V) with XANES edge positions for all the samples (17171.2 eV – 17169.6 eV) between those of U(VI) (17173.4 eV) and U(IV) (17170.3 eV). Additionally, shifts in the U L_{III}- edge XANES post-edge resonance features to a lower energy relative to the uranyl (U(VI)) standard indicate lengthening of the U-O_{axial} bonds and formation of a distorted uranate-like coordination consistent with the reported U coordination within magnetite (Figure S6).[30]

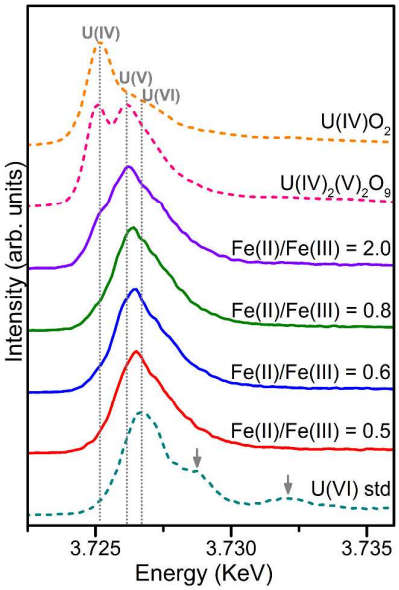

Figure. 1: U M4 HR-XANES of U co-precipitated with magnetite (Fe(II)/Fe(III) = 0.5 and 0.6) and green rust (Fe(II)/Fe(III) = 0.8 and 2.0) with standards $U(IV)O_2$[29], $U(IV)_2U(V)_2O_9$[29] and U(VI) adsorbed to ferrihydrite. Grey arrows indicate characteristic U(VI) features.

U incorporation within magnetite and green rust. U L_{III}–edge EXAFS spectra (Figure S7, Table S2) were analysed to determine the molecular scale speciation of U associated within the magnetite and green rust mineral phases. For U associated with magnetite (Fe(II)/Fe(III) = 0.5 and 0.6), the best fits confirm 4-4.5 oxygen backscatterers at 2.17(1)Å, indicative of uranate-like coordination,[1,2,8,9,12,30] which is consistent with our interpretation of the L_{III}–edge XANES spectra. The lower U-O coordination number than would be predicted for an octahedral site (i.e. <6), is due to the presence of a proportion of $U(IV)O_2$ or U(VI) within the sample. The fitting of Fe shells to the EXAFS was then informed assuming that U incorporation into magnetite occurred by substituting U for Fe at an octahedrally coordinated Fe site. The fits confirmed the presence of two U-Fe shells at 3.20(2) Å and 3.72(2) Å for Fe(II)/Fe(III) = 0.5 and 3.15 (2) Å and 3.69 (3) Å for Fe(II)/Fe(III) = 0.6, showing a systematic and significant increase in the interatomic distance relative to the Fe-Fe distances in magnetite (2.97 Å and 3.48 Å respectively[31]). In Fe(II)/Fe(III) = 0.6, the additional U-O and U-U backscattering shells observed at 2.42(3) Å and 3.89(2) Å respectively, reflect the presence of U(IV) supporting the HERFD-XANES data. Finally, the presence of 0.5 oxygen backscatterers at 1.81(2) Å in the fit for the Fe(II)/Fe(III) = 0.5 sample suggests a modest contribution from U(VI) in uranyl dioxygenyl coordination as confirmed by the ITFA

analysis, and which has been observed in past work on U(VI) sorption to magnetite surfaces.[1,8] .

For samples Fe(II)/Fe(III) = 0.8 and 2.0, the U-O coordination environment in green rust showed differences when compared to the magnetite system, with U-O distances at approximately 1.90 (6) Å and 2.17(1) Å again indicative of uranate-like coordination. Similar to the magnetite systems, additional U-O and U-U shells at ~ 2.46(2) Å and 3.89 (1) Å confirm the presence of uraninite (UO_2) as observed in past work.[16,32] Similar to the magnetite system, fitting of additional Fe shells was informed by the green rust structure and assumes direct substitution of octahedrally coordinated Fe by U. The best fits include 6 Fe at 3.09(1) Å and 3.28(2) Å with an additional shell of 4 Fe at 5.25(3) Å. These fits are consistent with the Fe-Fe distances in green rust, which are 3.19 Å and 5.52 Å respectively. Overall, the EXAFS confirm that U(V) is incorporated within octahedral sites in the Fe(II)/Fe(III) (oxyhydr)oxide phases in a uranate-like coordination environment. This is consistent with several recent experimental and theoretical reports showing U can directly substitute for octahedrally coordinated Fe in iron (oxyhydr)oxide mineral phases.[1,8,9,12,19] The current work extends these observations to systems where U(V) is the dominant species during direct precipitation of magnetite and green rust for the first time.

Mechanism of U(V) incorporation into magnetite and green rust.

Our results show that direct co-precipitation of U(VI) with magnetite and green rust leads to reduction to U(V) and subsequent stabilization within the bulk structure of both minerals. The stabilization of U(V) via incorporation into Fe(II)/Fe(III) bearing iron (oxyhydr)oxides has been hypothesised in several systems[1,8,9] with very recent work postulating U(V) stabilisation via incorporation into magnetite.[12] For the current work, in both systems U(V) is incorporated into the mineral structures via direct substitution of U for octahedrally coordinated Fe. In magnetite the average U(V)-O bond length is 2.17(1) (Fe(II)/Fe(III) = 0.5 and 0.6) consistent both with U(V) in uranate-like coordination[12,30] and also with recent atomistic simulations which predict a U-O distance of 2.08 Å for this system.[12,19,33] The U-Fe interatomic distances derived from the EXAFS data (i.e. 3.15-3.20 Å and 3.69-3.72 Å) are ≈0.2 Å longer than the Fe-Fe distances in magnetite (Table S2). Again these values are consistent with U(V) incorporation simulations for the first Fe shell (3.15 Å) in magnetite.[19] The reason for the increased interatomic distances is unlikely to be the size of the incorporated U(V) (the crystal radius for U(V) is 0.9 Å, and for Fe(II) / Fe(III) is 0.79 / 0.92 Å), rather increased repulsive electrostatic interactions between U(V) and the Fe(II/III) atoms pushed the iron out.[19]

The incorporation of U(V) into green rust (Fe(II)/Fe(III) 0.8 and 2.0) again occurs via direct substitution for octahedrally coordinated Fe within the sheet structure of the layered double hydroxide. Here, the EXAFS data indicate that the U(V) local coordination is different to that observed in magnetite (Figure S7). Indeed, the best fit for these samples confirmed 2 oxygens at ~1.9 Å, and a shell of 4 equatorial oxygens at 2.17 Å, again consistent with a uranate-like coordination environment (Table S2). This difference in the U(V)-O coordination in green rust relative to magnetite is presumably due to the layered structure of the green rust. Here, incorporation of U(V) within isolated octahedral sheets evidently provides significantly less steric constraint on the U(V)-O octahedron relative to U(V) in the highly constrained cubic spinel structure of magnetite. The variation in the axial and equatorial U-O bond lengths in the U(V) incorporated within green rust clearly leads to local distortion of

the green rust octahedral sheet and splitting of U-Fe distances relative to the Fe-Fe distances in green rust (Table S2). Overall, the best fit indicates three to four Fe-O octahedra adjacent to the short (1.9 Å) U-O axial oxygens, and approximately two Fe-O octahedra adjacent to the long (2.17 Å) U-O equatorial oxygens (Figure 2). This is consistent with the U(V) being present in a distorted environment and is presumably due to the enhanced flexibility of the octahedral sheet in green rust compared to the octahedral sites within magnetite. The novel incorporation of U(V) in green rust is in contrast to previous sorption studies where U(IV) surface complexes or $UO_{2(s)}$ were observed as the reaction end products.[16,32,34]

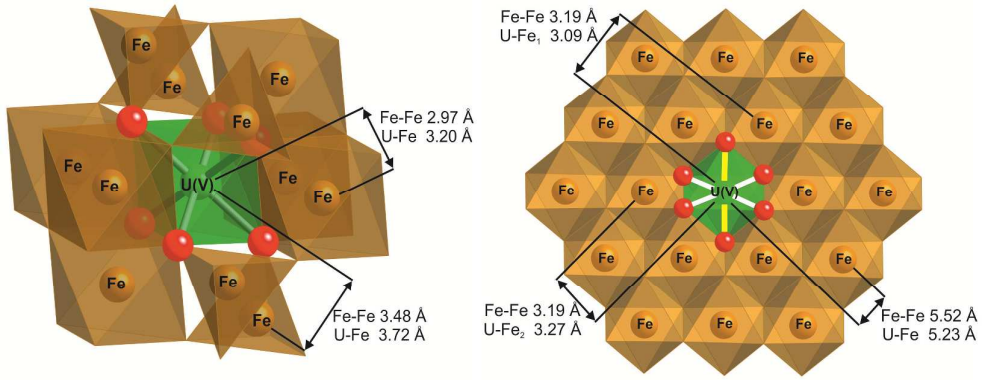

Figure. 2: (a) Magnetite structure showing Fe-Fe distances[31] and U-Fe distances obtained from EXAFS of Fe(II)/Fe(III) = 0.6; **(b)** Green rust structures showing Fe-Fe distances[35] and U-Fe distances obtained from EXAFS of Fe(II)/Fe(III) = 2.0. Yellow lines indicate shorter U-O distances (1.9 Å) and white lines indicate longer U-O distances (2.17 Å).

The observed energy shift of the U(V) M_4 HR XANES main peak position (Figure 1) for different Fe(II)/Fe(III) ratios (Figure S4) from 3726.5 eV (Fe(II)/Fe(III) = 0.5) to 3726.3 eV (Fe(II)/Fe(III) = 2.0) may relate to different strengths of the covalent bond between the U and neighbouring atoms.[36] Electronic structure calculations (Figure S8) show a clear difference in the distribution of density of states for U incorporated into the octahedral site of magnetite relative to green rust. The hybridization between U f-states and Fe d-states above the Fermi level are much stronger for U incorporated into green rust relative to magnetite. This may be associated with a stronger, more covalent, U bond in green rust compared to the U bond in the magnetite structure.

Mechanism of U(V) stabilization. Our results suggest that U(V) incorporation during magnetite and green rust formation occurs via a two-step process (abstract art): Firstly, U(VI) is adsorbed to the surface of the growing Fe(II)/Fe(III) (oxyhydr)oxide nanoparticles and undergoes reduction to U(V) via one electron transfer.[1] Secondly, during rapid crystal growth the U(V), which is compatible with the Fe octahedral site in both magnetite and green rust, becomes incorporated within the structure. Recent work has highlighted that disproportion of U(V) can occur on the magnetite surface, implying that stabilization of structural U(V) may only occur during rapid crystal growth rates.[5] Under these conditions, isolation of U(V) within the mineral structure seems to prevent its disproportionation to U(IV) and U(VI). Indeed, U(V) is reportedly stable for up to 550 days suggesting that incorporated U(V) may be stable over extended time periods.[8] Furthermore, steric constraints seem likely to favour U(V) stabilisation in these systems as U(IV) is incompatible

with octahedral sites as it requires a larger coordination environment (n = 8). Indeed, steric constraints may be the most crucial factor in stabilising U(V) as both magnetite and green rust are electrically conductive[37] and therefore physical isolation of U(V) alone seems unlikely to prevent disproportionation.

Implications for U speciation and fate in the environment

Here, we have shown the reduction of U(VI) to U(V) followed by incorporation into both magnetite and green rust is the dominant process during the direct precipitation of these mineral phases. The potential for U(V) incorporation processes to be dominant in these environmentally relevant phases is certainly highlighted in this and other very recent work[12] and has important, and as yet not fully explored implications for understanding and predicting U mobility in engineered and natural environments. Incorporation of U(V) into mineral phases commonly present in contaminated environments may offer a more resilient species to oxidative remobilisation compared to uraninite and adsorbed U(IV) which are readily oxidised to soluble U(VI) in many environmental systems.[9,38] The incorporation of U(V) in magnetite and green rust offers a promising prospect to optimise its incorporation in a range of engineered settings whilst the stability of U(V) in these systems clearly warrants further investigation.

Acknowledgements

This work was supported by the STFC (ST/L502534/1), ENV RAD NET (ST/K001787/1 and ST/N002474/1), and BIGRAD (NE/H007768/1).We thank both Diamond Light Source (SP9621-2, SP10163-1, SP12767-1) and European Synchrotron Radiation Facility (EV/192) for beamtime. We thank Dr Giannantonio Cibin and Dr Steve Parry for their help during beamtime at Diamond Light Source, Richard Doull for advice on radiological samples during beamtime at Diamond Light Source, Dr Sara Lafuerza for her help during beamtime at European Synchrotron Radiation Facility, Dr John Waters for help with XRD, Dr Heath Bagshaw for help with TEM, Ellen Winstanley for providing U(VI) data and Dr Carolyn Pearce for help with the mineral synthesis method.

References

(1) Ilton, E. S.; Boily, J. F. S.; Buck, E. C.; Skomurski, F. N.; Rosso, K. M.; Cahill, C. L.; Bargar, J. R.; Felmy, A. R. Influence of dynamical conditions on the reduction of UVI at the magnetite-solution interface. *Environ. Sci. Technol.* **2010**.

(2) Ilton, E. S.; Pacheco, J. S. L.; Bargar, J. R.; Shi, Z.; Liu, J.; Kovarik, L.; Engelhard, M. H.; Felmy, A. R. Reduction of U(VI) incorporated in the structure of hematite. *Environ. Sci. Technol.* **2012**.

(3) Massey, M. S.; Lezama-Pacheco, J. S.; Jones, M. E.; Ilton, E. S.; Cerrato, J. M.; Bargar, J. R.; Fendorf, S. Competing retention pathways of uranium upon reaction with Fe(II). *Geochim. Cosmochim. Acta* **2014**.

(4) Ilton, E. S.; Haiduc, A.; Cahill, C. L.; Felmyt, A. R. Mica surfaces stabilize pentavalent uranium. *Inorg. Chem.* **2005**, *44* (9), 2986–2988.

(5) Yuan, K.; Renock, D.; Ewing, R. C.; Becker, U. Uranium reduction on magnetite: Probing for pentavalent uranium using electrochemical methods. *Geochim. Cosmochim. Acta* **2015**, *156*, 194–206.

(6) Renshaw, J. C.; Butchins, L. J. C.; Livens, F. R.; May, I.; Charnock, J. M.; Lloyd, J. R. Bioreduction of uranium: Environmental implications of a pentavalent intermediate.

Environ. Sci. Technol. **2005**, *39* (15), 5657–5660.

(7) Yuan, K.; Ilton, E. S.; Antonio, M. R.; Li, Z.; Cook, P. J.; Becker, U. Electrochemical and spectroscopic evidence on the one-electron reduction of U(VI) to U(V) on magnetite. *Environ. Sci. Technol.* **2015**, *49* (10), 6206–6213.

(8) Huber, F.; Schild, D.; Vitova, T.; Rothe, J.; Kirsch, R.; Schäfer, T. U(VI) removal kinetics in presence of synthetic magnetite nanoparticles. *Geochim. Cosmochim. Acta* **2012**.

(9) Marshall, T. A.; Morris, K.; Law, G. T. W.; Mosselmans, J. F. W.; Bots, P.; Roberts, H.; Shaw, S. Uranium fate during crystallization of magnetite from ferrihydrite in conditions relevant to the disposal of radioactive waste. *Mineral. Mag.* **2015**, *79* (6), 1265–1274.

(10) Boland, D. D.; Collins, R. N.; Payne, T. E.; Waite, T. D. Effect of amorphous Fe(III) oxide transformation on the Fe(II)-mediated reduction of U(VI). *Environ. Sci. Technol.* **2011**.

(11) Boland, D. D.; Collins, R. N.; Glover, C. J.; Payne, T. E.; Waite, T. D. Reduction of U(VI) by Fe(II) during the Fe(II)-Accelerated Transformation of Ferrihydrite. *Environ. Sci. Technol.* **2014**.

(12) Pidchenko, I.; Kvashnina, K. O.; Yokosawa, T.; Finck, N.; Bahl, S.; Schild, D.; Polly, R.; Bohnert, E.; Rossberg, A.; Göttlicher, J.; et al. Uranium Redox Transformations after U(VI) Coprecipitation with Magnetite Nanoparticles. *Environ. Sci. Technol.* **2017**, No. Vi, acs.est.6b04035.

(13) Refait, P.; Genin, J. M. R. The oxidation of ferrous hydroxide in chloride-containing aqueous media and pourbaix diagrams of green rust one. *Corros. Sci.* **1993**, *34* (5), 797–819.

(14) Byrne, J. M.; Telling, N. D.; Coker, V. S.; Pattrick, R. A. D.; van der Laan, G.; Arenholz, E.; Tuna, F.; Lloyd, J. R. Control of nanoparticle size, reactivity and magnetic properties during the bioproduction of magnetite by Geobacter sulfurreducens. *Nanotechnology* **2011**, *22* (45), 455709.

(15) O'Loughlin, E. J.; Larese-Casanova, P.; Scherer, M.; Cook, R. Green Rust Formation from the Bioreduction of γ–FeOOH (Lepidocrocite): Comparison of Several Shewanella Species. *Geomicrobiol. J.* **2007**, *24* (Ii), 211–230.

(16) Dodge, C. J.; Francis, A. J.; Gillow, J. B.; Halada, G. P.; Eng, C.; Clayton, C. R. Association of uranium with iron oxides typically formed on corroding steel surfaces. *Environmental Science and Technology*. 2002.

(17) Tremaine, P. R.; LeBlanc, J. C. The solubility of magnetite and the hydrolysis and oxidation of Fe2+ in water to 300??C. *J. Solution Chem.* **1980**.

(18) Musić, S.; Ristić, M. Adsorption of trace elements or radionuclides on hydrous iron oxides. *J. Radioanal. Nucl. Chem. Artic.* **1988**.

(19) Kerisit, S.; Felmy, A. R.; Ilton, E. S. Atomistic simulations of uranium incorporation into iron (hydr)oxides. *Environ. Sci. Technol.* **2011**, *45* (7), 2770–2776.

(20) Pearce, C. I.; Qafoku, O.; Liu, J.; Arenholz, E.; Heald, S. M.; Kukkadapu, R. K.; Gorski, C. A.; Henderson, C. M. B.; Rosso, K. M. Synthesis and properties of titanomagnetite (Fe 3-xTi xO 4) nanoparticles: A tunable solid-state Fe(II/III) redox system. *J. Colloid Interface Sci.* **2012**.

(21) Burke, I. T.; Mosselmans, J. F. W.; Shaw, S.; Peacock, C. L.; Benning, L. G.; Coker, V. S. Impact of the Diamond Light Source on Research in Earth and Environmental Sciences: Current Work and Future Perspectives. *Phil. Trans. R. Soc. A* **2014**.

(22) Dent, A. J.; Cibin, G.; Ramos, S.; Smith, A. D.; Scott, S. M.; Varandas, L.; Pearson, M. R.; Krumpa, N. A.; Jones, C. P.; Robbins, P. E. B18: A core XAS spectroscopy beamline for

Diamond. *Journal of Physics: Conference Series*. 2009.
(23) Ravel, B.; Newville, M. ATHENA, ARTEMIS, HEPHAESTUS: Data analysis for X-ray absorption spectroscopy using IFEFFIT. In *Journal of Synchrotron Radiation*; 2005.
(24) Gauthier, C.; Solé, V. A.; Signorato, R.; Goulon, J.; Moguiline, E. The ESRF beamline ID26: X-ray absorption on ultra dilute sample. *J. Synchrotron Radiat.* **1999**, *6*, 164–166.
(25) Glatzel, P.; Bergmann, U. High resolution 1s core hole X-ray spectroscopy in 3d transition metal complexes - Electronic and structural information. *Coord. Chem. Rev.* **2005**, *249* (1–2), 65–95.
(26) Kvashnina, K. O.; Scheinost, A. C. A Johann-type X-ray emission spectrometer at the Rossendorf beamline. *J. Synchrotron Radiat.* **2016**, *23* (3), 836–841.
(27) Rossberg, A.; Ulrich, K. U.; Weiss, S.; Tsushima, S.; Hiemstra, T.; Scheinost, A. C. Identification of uranyl surface complexes on ferrihydrite: Advanced EXAFS data analysis and CD-music modeling. *Environ. Sci. Technol.* **2009**, *43* (5), 1400–1406.
(28) Vitova, T.; Kvashnina, K. O.; Nocton, G.; Sukharina, G.; Denecke, M. A.; Butorin, S. M.; Mazzanti, M.; Caciuffo, R.; Soldatov, A.; Behrends, T.; et al. High energy resolution x-ray absorption spectroscopy study of uranium in varying valence states. *Phys. Rev. B* **2010**, *82* (23).
(29) Kvashnina, K. O.; Butorin, S. M.; Martin, P.; Glatzel, P. Chemical state of complex uranium oxides. *Phys. Rev. Lett.* **2013**.
(30) Soldatov, A. V.; Lamoen, D.; Konstantinović, M. J.; Van den Berghe, S.; Scheinost, A. C.; Verwerft, M. Local structure and oxidation state of uranium in some ternary oxides: X-ray absorption analysis. *J. Solid State Chem.* **2007**.
(31) Fleet, M. E. The structure of magnetite. *Acta Crystallographica Section B Structural Crystallography and Crystal Chemistry*. 1981.
(32) O'Loughlin, E. J.; Kelly, S. D.; Cook, R. E.; Csencsits, R.; Kemner, K. M. Reduction of uranium(VI) by mixed iron(II)/iron(III) hydroxide (green rust): formation of UO2 nanoparticles. *Environ. Sci. Technol.* **2003**, *37* (4), 721–727.
(33) Shuller-Nickles, L.; Bender, W.; Walker, S.; Becker, U. Quantum-Mechanical Methods for Quantifying Incorporation of Contaminants in Proximal Minerals. *Minerals* **2014**, *4* (3), 690–715.
(34) Latta, D. E.; Boyanov, M. I.; Kemner, K. M.; Loughlin, E. J. O.; Scherer, M. Reaction of Uranium (VI) with Green Rusts : Effect of Interlayer Anion. **2015**, No. Vi, 156–168.
(35) Simon, L.; François, M.; Refait, P.; Renaudin, G.; Lelaurain, M.; Génin, J. M. R. Structure of the Fe(II-III) layered double hydroxysulphate green rust two from Rietveld analysis. *Solid State Sci.* **2003**, *5* (2), 327–334.
(36) Neidig, M. L.; Clark, D. L.; Martin, R. L. Covalency in f-element complexes. *Coord. Chem. Rev.* **2013**, *257* (2), 394–406.
(37) Hubbard, C. G.; West, L. J.; Rodriguez-Blanco, J. D.; Shaw, S. Laboratory study of spectral induced polarization responses of magnetite — Fe 2 redox reactions in porous media.
(38) Finch, R. J.; Ewing, R. C. The corrosion of uraninite under oxidizing conditions. *J. Nucl. Mater.* **1992**, *190* (C), 133–156.